JOURNAL OF CATALYSIS 132, 440–450 (1991)

Reduction of Nitric Oxide by Ammonia at Atmospheric Pressures over Platinum Polycrystalline Foils as Model Catalysts

T. KATONA,*,†,‡ L. GUCZI,*,§ AND G. A. SOMORJAI*,†

*Materials and Chemical Sciences Division, Center for Advanced Materials, Lawrence Berkeley Laboratory, 1 Cyclotron Road, Berkeley, California 94720; †Department of Chemistry, University of California, Berkeley, California 94720; ‡Department of Organic Chemistry, Jozsef A. University, Dom ter 8, Szeged, H 6720 Hungary; and §Institute of Isotopes, Hungarian Academy of Sciences, P.O. Box 77, Budapest, H 1525 Hungary

Received April 8, 1991

The reduction of nitric oxide with ammonia was studied using batch-mode and flow-mode measurements in partial pressure ranges of 70–660 Pa (0.5–5 Torr) on polycrystalline platinum foils over the temperature range of 373–633 K. The reaction products observed were nitrogen, nitrous oxide, and water. Unimolecular decompositions of NO or NH_3 were not detectable under these conditions, up to 773 K. The reduction of nitric oxide with ammonia occurred in the temperature range of 548–633 K. The Arrhenius curve of the reaction showed a break in the 563–603 K range, which was slightly dependent on the reactant concentrations. In this temperature range the reaction became oscillatory. The activation energies were 102 kJ/mol in the low-temperature and 212 kJ/mol in the high-temperature ranges, respectively. The product distribution was different in the two temperature regions; in the low-temperature range the N_2/N_2O ratio was close to 1, while in the high-temperature regime N_2 formation was dominant, and the previously formed N_2O was consumed as well.

INTRODUCTION

Combustion of carbon or hydrocarbons in the 1500–1800 K temperature range that is usually employed can lead to the formation of substantial amounts of nitrogen oxides (10–10^3 ppm) (*1, 2*) by direct reactions between nitrogen and oxygen. Many studies (*3, 4*) have been carried out on the catalytic removal of NO, and ammonia is an effective reducing agent according to the reactions

$$4NH_3 + 6NO \rightarrow 5N_2 + 6H_2O \quad (1)$$

$$2NH_3 + 8NO \rightarrow 5N_2O + 3H_2O. \quad (2)$$

The catalyst frequently used commercially to perform these reactions is vanadium oxide–titanium oxide (*5*). The kinetics of NO reduction on these oxides have been studied in some detail (*6*). It should be noted that the reaction is carried out in excess oxygen (*7*) (typically 0–1% O_2; 0–1000 ppm NO and NH_3; T = 673–873 K), and thus the surface conditions of the catalysts reflect the highly oxidizing conditions.

Platinum, an excellent oxidation catalyst may also be used for NO reduction by ammonia in the presence of excess oxygen. It promises to have much higher turnover rates than the transition metal oxides and it is worthy of exploration in depth for this purpose. This is the aim of our studies. We use ≃2-cm^2 surface area polycrystalline foils of platinum as model catalysts. The surface is cleaned and characterized by UHV surface science techniques. Then, it is enclosed in a reaction cell that can be pressurized to reach atmospheric pressure and the NO + NH_3 reaction is studied by measuring the rates of the reaction as a function of temperature and reactant pressures.

Our studies of the NO/NH_3 reaction over platinum are divided into two parts: (a) studies in the absence of oxygen and (b) studies in excess oxygen. In this paper we report the kinetics of this reaction in the absence

0021-9517/91 $3.00

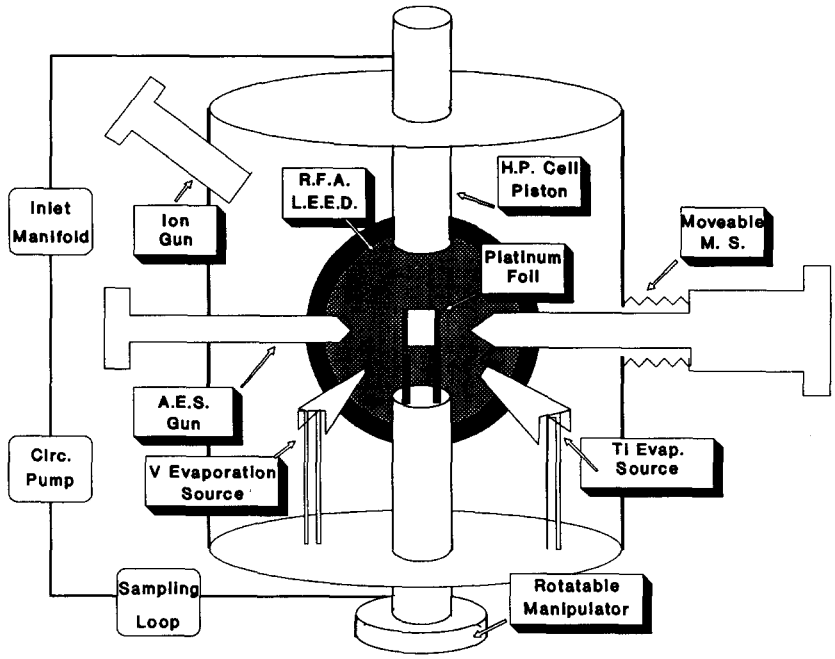

FIG. 1. Schematic diagram of the UHV chamber equipped with the high-pressure cell.

of oxygen. Detailed kinetic studies of the oxygen-containing reaction system will be reported elsewhere. Our studies were carried out in the 373–633 K temperature range using 70–650 Pa (0.5–5 Torr) partial pressure range for the reactant gases. The reaction rates were measured both in the batch mode and flow mode.

EXPERIMENTAL

A. Apparatus

The measurements were carried out in a low-pressure, high-pressure system designed for combined surface analysis and catalytic studies using small area samples. The schematic diagram of the apparatus is shown in Fig 1. Using this system the Pt samples were prepared and characterized under ultrahigh-vacuum (UHV) conditions and then isolated from the main chamber by the use of the high-pressure cell, which is connected to a recirculation loop that can be used as a batch reactor for high-pressure catalytic experiments. It is also possible to use this reactor in flow mode when the reaction mixture passes the catalyst once without recirculation. After the reaction, the high-pressure cell can be evacuated and reopened in order to carry out further surface characterization without exposing the sample to air.

The main vacuum system consisted of a stainless-steel chamber that was pumped by a high-speed oil diffusion pump (Varian VHS 6) equipped with a liquid nitrogen trap (Varian 362-6). A base pressure of $6–10 \times 10^{-8}$ Pa ($5–8 \times 10^{-10}$ Torr) was achieved after 24 h bake out at 373 K. The background consisted of mostly CO, CO_2, H_2O, and air from a virtual leak in the sample manipulator. The chamber was equipped with a nude ion gauge (Varian 971-5008) for pressure measurements; an ion sputtering gun (PHI 4-161) for sample cleaning; a quadrupole mass spectrometer (MS) (UTI 100C) for gas analysis, which was mounted on bellows and equipped with a tubular guide for temperature-programmed desorption spectroscopic (TDS) studies; a homemade Auger electron gun; and a four-grid electron optics

retarding field energy analyzer (RFA) (Varian 981-0127) for Auger (AES) and low-energy electron diffraction (LEED) studies. There were two evaporative metal sources (Ti and V) built in the chamber for later use as well.

The manipulator, which allowed rotational movement, consisted of two copper rods ending with small Pt pieces that held the sample. The 2-cm^2 area 0.0254-mm-thickness Pt foil was spot welded to 0.254-mm gold wires, which were spot welded to these Pt pieces. The foil was heated resistively by applying a current to the copper rods. A chromel–alumel thermocouple was spot welded to the bottom edge of the sample. The temperature was calibrated using an optical pyrometer. The copper rods were hollow, which allowed cooling either with liquid nitrogen for TDS or air flow for catalytic measurements.

The manifold system was constructed of stainless-steel 6.35-mm-diameter tubes and stainless-steel ball valves (Nupro SS 421). Reactant gases were introduced via flow meters (Matheson FM 1051B). Pressure was measured by Wallace–Tiernan gauges (FA 160, FA 20). The manifold was pumped with a mechanical pump followed by liquid nitrogen-cooled sorption pumps. The reactant mixture was circulated with a teflon-lined circulation pump (Fluorocarbon GP 21B) that contained no metallic part in the way of the gases. The highest flow rate that we obtained using this pump was approximately 250 cm^3/min. Sequentially introduced reactants were mixed after 2 min according to MS analysis.

A six-way sampling valve was incorporated into the reactor exit tube. The sampling loop consisted of a photo ionization detector (PID) (HNU), which was only sensitive for the NO in the reaction mixture, and thus no separation was necessary. We used this detector for our early measurements and for calibration the performance of our MS. GC analysis was also carried out using this sampling valve. We obtained proper separation of Ar, N_2, O_2, NO, N_2O, and NO_2 on a 6-m Hayesep D polymer column at 308 K, but NH_3 and H_2O wee irreversibly adsorbed. Since the time of the analysis was long compared to the time of the reaction, we used MS analysis for the kinetic studies.

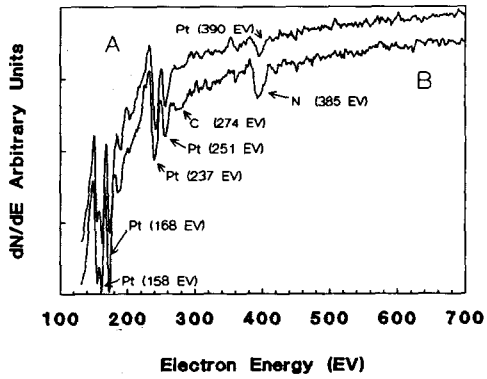

FIG. 2. Auger spectra of Pt foils. (A) Spectrum of cleaned sample before the reaction; (B) after the reaction. The only surface components that can be detected by AES except of Pt are N (385 EV) and C (272 EV).

B. Gases

For the reaction 1% NO in helium, 1% NH_3 in helium, 1% O_2 in helium, and 1% Ar in helium (Matheson certified standards) were used without further purification. For the ion sputtering and oxygen treatment high-purity Ar and O_2 (Airco) were used respectively. High-purity NH_3, N_2O, NO, NO_2, N_2, and O_2 gases were used for calibration.

C. Sample Preparation

Platinum samples were cleaned by subsequent ion sputtering (6.65×10^{-3} Pa (5×10^{-5} Torr) Ar, 2 kV, 30 mA, 15 μA) and O_2 annealing (973 K, 1.33×10^{-4} Pa (1×10^{-6} Torr)). The cleanliness of the surface was monitored by AES (15-mA emission, 2 KV, 60-μA incident current with a 3-mm-diameter defocused beam, 5-V modulation, 50 V/min sweep). The Auger spectrum of the cleaned sample is shown in Fig. 2A.

D. Experimental Procedure

After cleaning the sample, the high-pressure cell was closed, the circulation pump

was started, and the reactants were introduced into the reaction loop via the flow meters, using a pressure gauge to measure the introduced amounts. Since our reactants were in 1% concentration in He balance, pressure was measured in 0- to 103-kPa (0–760 Torr) scale with accuracy of 650 Pa (5 Torr); this resulted in high accuracy and reproducibility at setting initial partial pressures. It was possible to introduce pure gases using auxiliary valves when higher partial pressures were used. In those cases, a low-pressure gauge was used with accuracy of 13.3 Pa (0.1 Torr), and the reaction loop was filled up with He to obtain 103 kPa (760 Torr). All the reactions were run at a total pressure of 103 kPa (760 Torr) in order to obtain the same circulation speed. Most of the experiments were carried out using nonhelium compounds with total pressure of 1.03 kPa (7.6 Torr).

We applied MS analysis to determine gas-phase concentrations in the reaction mixture. Instead of using separate leak valve to introduce gases into the UHV chamber we utilized the leak that occurred at the sealing of the high-pressure cell. We modified the hydraulics of the high-pressure cell closing system in order to achieve fine adjustment of this leak. Since the sum of the partial pressures of the reactants was 1% of the total pressure, 2.66×10^{-4} Pa (2×10^{-6} Torr) was set in the UHV chamber in order to get compounds partial pressures in the 10^{-6} Pa (10^{-8} Torr) range. We assumed that because of the high dilution of the mixture, the sensitivity of the ion gauge did not depend on the composition. We also used Ar, as an internal standard in the reaction mixture in the same partial pressure range as the other compounds. Using the intensity at AMU 40 for Ar and assuming that it is proportional to the leak rate into the chamber, we could eliminate the uncertainty due to the poor reproducibility of the setting of the background pressure and any changes in the pressure in the chamber during the reaction. Calibration was carried out for all of the compounds. Intensities were normalized to the Ar internal standard. Multiple fragmentation patterns were taken into account as well as background intensities.

The MS was connected to a programmable peak selector (PPS) (UTI 2064), which allowed the use of the selected ion monitoring (SIM) technique. Usually, eight peaks were monitored continuously. The PPS was on-line connected to an IBM compatible PC via serial communication adapter. The sampling cycle, during which the PPS read all the preset intensities and sent them to the PC, was approximately 6 s.

Four minutes after the reaction mixture had been introduced and 2.66×10^{-4} Pa (2×10^{-6} Torr) was set in the chamber, the MS–PPS analysis was started and peak intensities were recorded for 1 min in order to determine initial concentrations in the reaction loop. Then the catalyst was heated to the desired temperature, which was reached within ± 1 K in 1 min using precision temperature controller. The copper rods of the manipulator were cooled applying air flow through them. During the reaction the peak intensities were continuously recorded. At the end of the reaction the reaction loop was pumped down. During this period, peak intensities were also recorded in order to obtain background values for each recorded channels. The 10-bit resolution data were stored in ASCII files.

Gas-phase concentrations were calculated using data handling software. The accuracy of N_2, NO, and N_2O measurement was within 5%. In the case of NH_3 and H_2O, because of their strong adsorption capability, this accuracy was between $\pm 10\%$. Comparison of background data before and after the reaction showed that during the reaction both the NH_3 and H_2O related peaks were increased. Blank experiment was carried out using Au foil instead of Pt. We did not find background activity within the limits of our experimental detectability.

RESULTS

A. NH_3 and NO Decomposition

Within the limits of our selected ion monitoring mass spectrometric analysis, we did not find decomposition products either for

NH_3 or NO in the temperature range of 373–673 K and partial pressure ranges of 66–1010 Pa (0.5–7.6 Torr). These findings are in good agreement with literature data. Schmidt (*8*) and co-workers reported the appearance of the decomposition of ammonia above 773 K over Pt wires at pressures of 13–266 Pa (0.1–2 Torr). The decomposition is pressure independent at lower temperatures (773–1000 K) and becomes first order in the high-temperature region (1200–1500 K). Although the repeated experiments by the same group showed decomposition at lower temperatures (500 K) (*10*), we have no evidence for this from our studies. The decomposition reaction was reported to be strongly inhibited by H_2 on Pt, which supports the dissociative adsorption model as well as the temperature-programmed desorption studies, where NH_3 gave a broad desorption peak in the 170–400 K range (*21*).

Pignet and Schmidt (*8*), using the same NO pressure range, did not detect NO decomposition over Pt wires below 1000 K. The rate of decomposition was $\simeq 6 \times 10^{15}$ mol · s^{-1} · cm^{-2} at 1500 K. In a later experiment, where the temperature and pressure ranges were extended, Mummey and Schmidt (*23*) reported a nitric oxide decomposition rate of $\simeq 5 \times 10^{14}$ mol · s^{-1} cm^{-2} at 650 K using 133 Pa (1 Torr) NO in a batch-mode UHV high-pressure cell system over polycrystalline platinum foil. The NO decomposition was found pressure independent at low temperatures and high NO pressures.

TPD studies showed that NO gave multiple desorption peaks corresponding to associatively (300 K) and dissociatively (450 K) adsorbed species (*20, 21*). At 450 K the N_2 desorption peak and N_2 and N_2O formation were found on the Pt(111) surface (*21*) and polycrystalline Pt foils, respectively (*22*). Since NO decomposition was found to occur at remarkably higher temperatures in the high-pressure region, we can conclude that at higher coverages and lower temperatures it is strongly inhibited by chemisorbed NO itself.

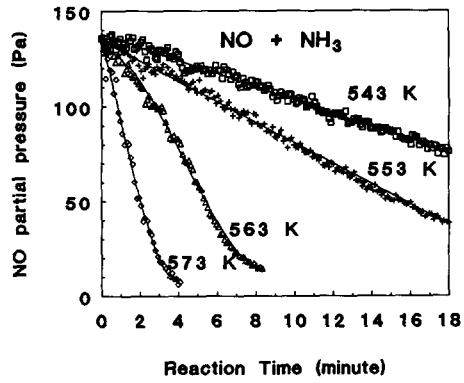

FIG. 3. Temperature dependence of NO consumption in batch mode using 133-Pa (1 Torr) NO and 400-Pa (3 Torr) NH_3 initial partial pressures. □ 543 K; + 553 K; △ 563 K; ◇ 573 K.

It has also been shown that NO can oxidize platinum above 773 K in UHV (*20*). Since the decomposition of NO was found above 1400 K at high pressures, we can conclude that in that case not only the Pt, but also the Pt–O system, should be considered as catalyst.

B. NH_3 + NO Reaction

1. Temperature dependence and product distribution. In the temperature range of 548–633 K, and partial pressures of 65–650 Pa (0.5–5 Torr) NO reacted with NH_3 on the platinum foil. The temperature dependence of the NO consumption is shown in Fig 3. Below 573 K the NO consumption is slower; above that temperature it accelerates. Above 633 K the reaction becomes too fast for batch mode measurements. The Arrhenius plot of the reaction is presented in Fig. 4. The two well-distinguishable portions of the curve, corresponding to the high-temperature faster reaction regime and the low-temperature slower process region, show $\Delta E_1^{\#} = 212$ kJ/mol and $\Delta E_2^{\#} = 102$ kJ/mol apparent activation energies, respectively. The position of the break point shows slight dependence on the NO partial pressure. At a given temperature, depending on the partial pressure of the NO, the rate of the reaction changes; this is shown in Fig. 5. The product

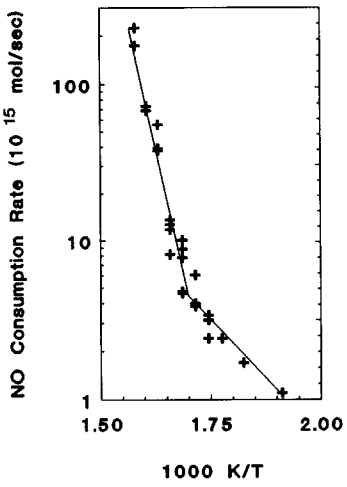

FIG. 4. Arrhenius plot of NO consumption using 480-Pa (3.6 Torr) NO and 400-Pa (3 Torr) NH_3 initial partial pressures. Each point represents one separate experiment. NO consumption rates are expressed in 10^{15} molecules/s.

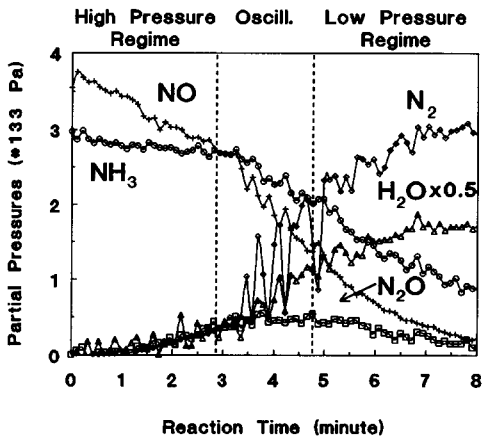

FIG. 6. Reactants and product partial pressure changes during the reaction at 593 K and at 480-Pa (3.6 Torr) NO and 400-Pa (3 Torr) NH_3 initial partial pressures. + NO; ○ NH_3; ◇ N_2; □ N_2O; △H_2O.

distribution is also different in the two regions (Fig 6). At lower temperatures and/or high NO partial pressures, next to the slow N_2 formation, N_2O formation was also monitored giving an N_2/N_2O ratio close to 1. When the NO partial pressure decreased below a well-defined value, apparently a sudden change in the reaction pattern took place, i.e., the rate of N_2 formation was increased, and the N_2O, which formed previously in the course of the reaction, was consumed. The transition from the high-pressure/low-temperature regime to the low-pressure/high-temperature region gave rise to oscillation (Fig. 6). In the low-pres-

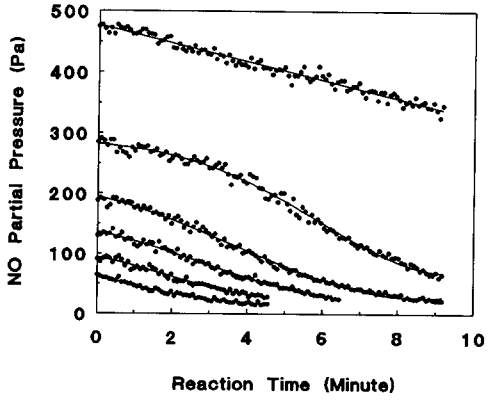

FIG. 5. Effect of the initial NO partial pressure on the rate of NO consumption in batch mode at 583 K. The initial NO partial pressures are: 480, 300, 200, 133, 100, and 66 Pa.

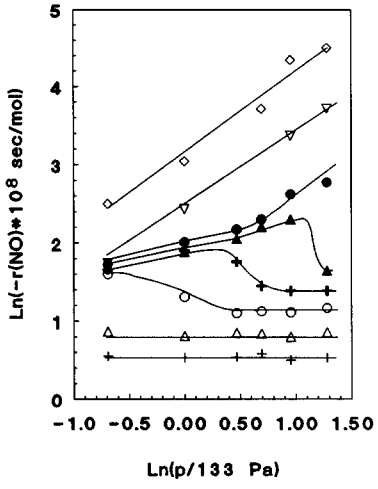

FIG. 7. Effect of NO initial partial pressure on the NO consumption rate at various temperatures: $\mathrm{Ln}(-d(\mathrm{NO})/dt \times 10^8\ \mathrm{s} \cdot \mathrm{mol}^{-1})$ vs $\mathrm{Ln}(p)$ plot. + 548 K; △ 563 K; ○ 573 K; + 583 K; ▲ 593 K; ● 603 K; ▽ 613 K; ◇ 623 K.

sure/high-temperature region mostly N_2 formation was detected, the N_2/N_2O ratio was found to be between 10 and 15.

Results of reaction order studies for NO are shown in Fig. 7 at different temperatures. At lower temperatures clear zero-order behavior can be seen. At 573 K, when NO partial pressure drops below 200 Pa (1.5 Torr), the NO consumption rate jumps and a different reaction pattern emerges (refer to Fig. 7). At 613 K and above, the initial NO consumption rates show first-order kinetics with respect to initial NO pressures. This change in the reaction patterns occurs in a relatively narrow (50 K) temperature range, and the separation point between the two reaction paths shifts toward higher temperatures with higher NO partial pressures.

Reaction order studies for NH_3 showed zero-order kinetics in the low-temperature region and half order in the high-temperature range (Fig. 8). Its reaction order seemed to be connected closely to the NO pressure-dependent reaction patterns; i.e., the half-order kinetics appeared only when NO showed first-order behavior.

2. Oscillation. In the temperature range of 573–613 K, depending on the NO partial pressure, two different reaction patterns with activation energies of 102 and 212 kJ/mol, reaction orders of zero for both reactants in the low-temperature region and first and half orders in the high-temperature regime for the NO and ammonia can be obtained. At a certain temperature, as the reaction proceeds, and NO is consumed, the NO partial pressure decreases below a certain value and oscillation starts.

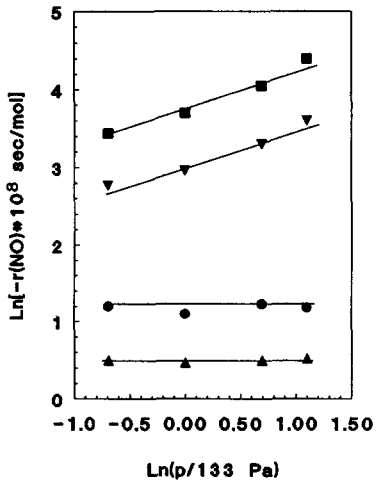

FIG. 8. Effect of NH_3 initial partial pressure on the NO consumption rate at various temperatures: $\mathrm{Ln}(-\,d(\mathrm{NO})/d\,t = 10^8\ \mathrm{s}\cdot\mathrm{mol}^{-1})$ vs $\mathrm{Ln}(p)$ plot. ▲ 548 K; ● 573 K; ▼ 613 K; ■ 623 K.

It should be noted that due to the geometry of the high-pressure cell, the gas mixture that leaves the catalyst area is sampled via the leak of the high-pressure cell gasket; thus our reactor can be considered as a flow reactor where the whole gas stream is fed back. In most of the cases when the reaction rate is slow and conversion is low, standard batch reactor behavior can be assumed; however, in the case of oscillation, when sudden and considerable changes appear in the reactant concentrations, the apparent intensities are related only to the portion of the gas stream that leaves the catalyst.

The oscillatory behavior was also studied in standard steady-state flow mode where reaction mixture was vented after having passed the catalyst area. (The flow rate we used was between 150 and 450 cm^3/min. Assuming plug-like stream, the gas residence time in the catalyst volume was at least two orders of magnitude less than the cycle time of the oscillations we obtained.)

In Fig. 9 oscillation obtained in flow mode is shown. It starts when the temperature is raised by 10 K from 593 to 603 K. Referring to Fig. 7, this is the temperature and pressure region, where the 10 K increase in the temperature shifts the reaction system from one regime to another. It is also seen that there is an induction period when smaller amplitude cycles appear, then the oscillation reaches its "steady state." Once started it can be maintained for hours. In Fig. 9 the mass spectrometric intensities of the Ar internal standard are also plotted showing that the gas flow through the reactor is uniform, the observed fluctuations in the reactant concentrations are due only to the chemical reaction, and no turbulences

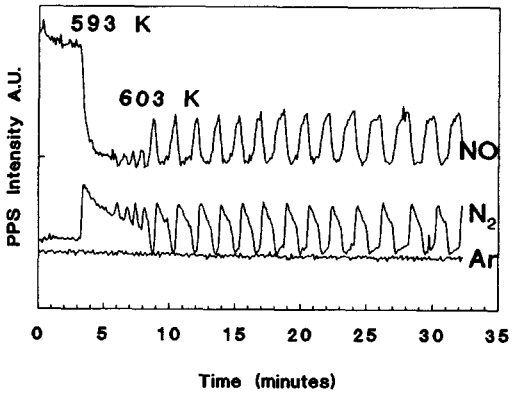

FIG. 9. Oscillation in flow mode at 603 K. Initial partial pressures are P_{NO} = 440 Pa (3.3 Torr); P_{NH_3} = 440 Pa (3.3 Torr); P_{Ar} = 133 Pa (1 Torr). Flow rate: 150 cm^3/min. PPS intensities in arbitrary units are plotted vs time.

occur. In Figs. 10A and 10B oscillation is shown at 623 K. At higher temperature the cycle time is shorter.

The changes in the NO, N_2, and N_2O concentrations during the oscillation are shown on Fig. 11 using mass spectrometric intensities in arbitrary units. Where the NO concentration peaks, the rate of the reaction is the lowest. Along dashed line A NO partial pressure is high, N_2 formation is slow, and there is a considerably high amount of N_2O forming. (MS intensities are plotted in arbitrary units and adjusted in scale for better view.) Referring to Figs. 6 and 7, this point clearly belongs to the high-pressure reaction pattern (refer to Fig. 6). While NO concentration drops, N_2 formation jumps along dashed line B, and at the same time the formation of N_2O drops to its lowest value. The sudden changes are clearly seen in the concentrations of N_2 and N_2O, while the NO curve is smoother. This is due to the slower pumping speed of our vacuum system for NO. Dashed line B represents the low-NO-pressure portion of the reaction system in Figs. 7 and 6. Between dashed line B and C, N_2 formation rate slowly decreases, while N_2O formation rate concertedly increases and NO concentration remains around its lowest value. In this regime both reaction paths exist but N_2O production is taking over, as compared to N_2 formation. At dashed line C, N_2 formation sharply drops to its lowest value, and NO consumption decreases, showing high partial pressure in the gas phase. N_2O formation keeps its increasing trend, and at dashed line E reaches its highest value. At this point the cycle is started again.

DISCUSSION

Let us summarize our findings of our kinetic studies of the NO/NH_3 reaction that aids the elucidation of the mechanism of the catalytic process.

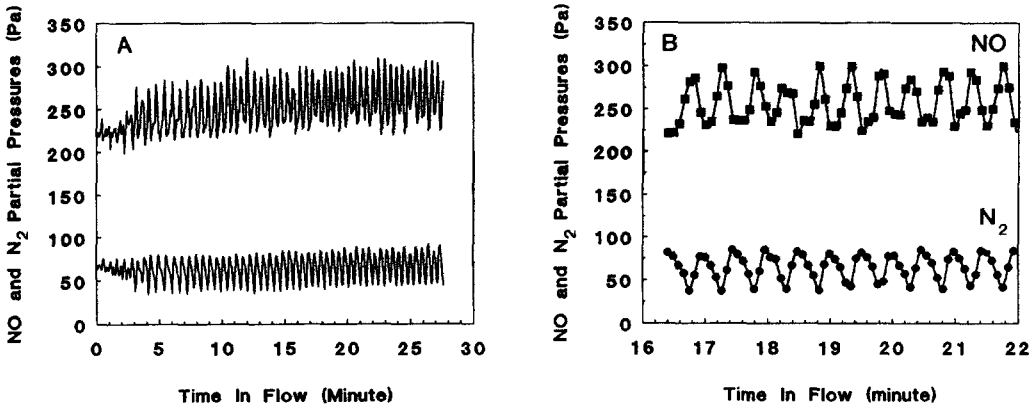

FIG. 10. Oscillation in flow-mode at 623 K. (A) Initial partial pressures and flow rate are the same as those in Fig. 9. (B) Shows sampling points over a zoomed portion of (A).

(1) In the temperature range of 573–613 K of our study there is a break in the Arrhenius curve. In the low-temperature region $\Delta E^{\#} =$ 102 kJ/mol, in the high-temperature regime $\Delta E^{\#} = 212$ kJ/mol apparent activation energies are found. The products we observe are N_2, N_2O, and H_2O. In the low-temperature region the N_2/N_2O ratio is close to 1, and at high-temperature the dominant product of the reaction is N_2.

(2) In the pressure regime (65–650 Pa, 0.5–5 Torr) of our study the reaction is zero order in NO in the temperature range of 548–573 K, and first order in NO in the 603–633 K range. The reaction rate is zero order in NH_3 partial pressure in 548–573 K range and half order in the 603–633 K range.

(3) In the temperature range of 573–623 K, where transition from one reaction regime to the other occurs, the reaction rate oscillates. The oscillation is accompanied by periodic change in the product distribution.

Our finding in the low-temperature region is in agreement with Otto *et al.*'s results (*13*). They obtained somewhat higher reaction rate at lower temperature using supported Pt catalysts, but the N_2O selectivity was similar to that we monitored. The zero-order kinetics we observe is reasonable at these high coverages and low temperatures.

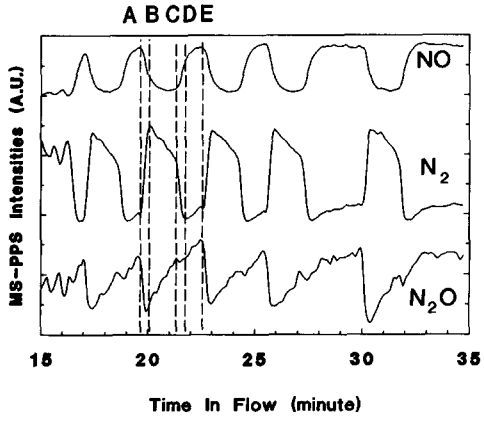

FIG. 11. Oscillation at 603 K in flow mode—changes in product distribution. Mass spectrometric intensities are plotted in arbitrary units.

The apparent activation energy related to the low-temperature region is also in the range of literature data.

In the temperature range of 423–473 K using relatively high partial pressures of isotope-labeled compounds they showed that the nitrogen product of the reaction was isotopically mixed due to the reaction of NO and NH_x species. The N_2/N_2O ratio they found was 1, which is in agreement with our finding in the low-temperature/high-pressure regime. They also found kinetic isotope effect using ND_3 and concluded that the rate-limiting step of the reaction involved the dissociation of the ammonia (*17*). This was interpreted by Pusateri *et al.* as a result of the high reaction rate and coverage under those conditions (*11*). Their observed N_2/N_2O ratio using supported platinum catalysts at temperatures the same as those used by Otto and co-workers was close to 2 at lower NO partial pressures. However, in the temperature range of 423–473 K and at pressures of 250–1000 Pa, the reaction rate was first order with respect to NO and half order with respect to NH_3, in agreement with the results of Tsai and co-workers (*18, 19*).

In UHV the reaction was studied by Gland and Korchak (*7*). The reaction occurred in the 423–773 K range. Under UHV conditions no N_2O formation was observed. The reaction showed first-order behavior in NO and half-order behavior in NH_3.

Takoudis and Schmidt (*9*) proposed a rate expression that could describe the N_2/N_2O ratio changes either in the high-pressure region or under UHV conditions. Using platinum wires and a well-stirred steady-state differential tank reactor, the N_2/N_2O ratio was found to be in the range of 3.5–20 and showed dependence on the reactant partial pressures and temperatures in accordance of the proposed rate expression.

According to Ref. (*9*) the N_2O formation rate depends mostly on the relative coverage of NO. At low temperatures and high NO partial pressures the relative population of HNO-S (*14*) species is higher; thus higher

N_2O formation rate can be monitored, but the sharp change in the reaction rate (Fig. 6) suggests a change in the mechanism as well, and cannot be described using simple Langmuir–Hinshelwood approximation. In the case of the oscillation steady-state treatment of the surface intermediate species may be in question.

We should point out that in the high-temperature/low-pressure region the reaction between NH_3 and N_2O has to be taken into account as well.

$$2NH_3 + 3N_2O = 4N_2 + 3H_2O. \quad (3)$$

We found first-order kinetics in NO partial pressure above 613 K. Pusateri *et al.*, using supported platinum catalyst, found the same NO order at somewhat lower temperatures (*11*). Schmidt (*14*), on the other hand, reported strong NO inhibition even at 873 K. Their reaction rate was considerably higher with turnover frequencies up to 100 s^{-1} (assuming $10^{16}/cm^2$ Pt atoms on the surface of a Pt wire), while Pusateri's results gave TOFs between 0.03 and 0.5. Thus our results, with TOFs in the range of 0.1–10 s^{-1} can be placed in between. It should be noted that the rate expression given by Takoudis and co-workers can predict oscillation (*14–16*). However, the model that treats the oscillation gave acceptable results only in those cases when bulk phase mass balance was taken into account. In our case, the amplitude of the oscillation was about 10 times higher (conversion was about 15%); i.e., no differential behavior could be assumed, and mass transfer limitation could occur as well. However, the overall reaction rate values did not show dependence on the gas velocity; thus we believe that our system was run in the kinetic regime. Detailed kinetic study of the oscillation including investigation of the transient behavior of our reactor system is to be reported elsewhere.

SUMMARY

The reaction system of NH_3 and NO was studied over polycrystalline Pt foils in the temperature range of 373–633 K at atmospheric total pressure using reactant partial pressures in the range of 70–650 Pa. In this pressure and temperature range no NO or NH_3 decomposition reaction occur, while the reaction between the NH_3 and NO proceeds rapidly. The only products we observed were N_2, N_2O, and H_2O. Using batch-mode measurements two well-distinguishable reaction patterns can be identified. The low-temperature/high-NO-partial-pressure regime shows zero reaction order with respect of both of the reactants, while in the high-temperature/low-NO-partial-pressure range first- and half-order kinetics with respect to NO and NH_3 are found, respectively. The two reaction regimes are divided by a transition range where the reaction rate oscillates. This sustained phenomenon was strongly dependent on the temperature and reactant mixture and was reproducible on many foils. Product distribution changes can be explained on the basis of fluctuation between the two observed reaction patterns.

ACKNOWLEDGMENTS

This work was supported by the Director, Office of Energy Research, Office of Basic Energy Sciences, Materials Science Division, U.S. Department of Energy, under Contract No. DE-AC03-76SF0098. The authors thank Johnson Matthey Co. for financial support.

REFERENCES

1. Youn, K. C., *Hydrocarbon Process.* **58**(2), 177 (1979).
2. Newman, D. J., *Chem. Eng. Prog.* **67**(2), 79 (1971).
3. Klimish, R. L., and Taylor, K. C., *Environ. Sci. Technol.* **7**(2), 73 (1972).
4. Kobylinsky, T. P., and Taylor, W., *J. Catal.* **33,** 376 (1974).
5. Nonnenmacher, H., and Kartte, K., US Pat. 3,279,884 (1966).
6. van Tol, M. F. H., Quinlan, M. A., Luck, F., Somorjai, G. A., and Nieuwenhuys, B. E., *J. Catal.* **129,** 186 (1991).
7. Gland, J. L., and Korchak, V. N., *J. Catal.* **55,** 324 (1978).
8. Pignet, T., and Schmidt, L. D., *Chem. Eng. Sci.* **29,** 1123 (1974).
9. Takoudis, G. C., and Schmidt, L. D., *J. Phys. Chem.* **87,** 958 (1983).

10. Papapolymeru, G. A., and Schmidt, L. D., *Langmuir* **1,** 488 (1985).
11. Pusateri, R. J., Katzer, J. R., and Manogue, W. H., *AIChE J.* **20,** 219 (1974).
12. Bauerle, G. L., Wu, S. C., and Nobe, K., *Ind. Eng. Chem. Prod. Res. Dev.* **14**(2), 123 (1975).
13. Otto, K., Shelef, M., and Kummer, J. T., *J. Phys. Chem.* **75**(7), 875 (1971).
14. Takoudis, C. G., and Schmidt, L. D., *J. Phys. Chem.* **87,** 964 (1983).
15. Takoudis, C. G., and Schmidt, L. D., *J. Phys. Chem.* **87,** 969 (1983).
16. Nowobilsky, P., and Takoudis, C. G., *Chem. Eng. Comm.* **33,** 211 (1985).
17. Otto, K., Shelef, M., and Kummer, J. T., *J. Phys. Chem.* **74**(13), 2690 (1970).
18. Tsai, J., Agraval, P. K., Sullivan, D. R., Katzer, J. R., and Manogue, W. H., *J. Catal.* **61,** 192 (1980).
19. Tsai, J., Agraval, P. K., Sullivan, D. R., Katzer, J. R., and Manogue, W. H., *J. Catal.* **61,** 204 (1980).
20. Gland, J. L., and Sexton, B. A., *J. Catal.* **68,** 286 (1981).
21. Gland, J. L., and Collin, E. B., *J. Catal.* **68,** 349 (1981).
22. Katona, T., and Somorjai, G. A., to be published.
23. Mummey, M. J., and Schmidt, L. D., *Surf. Sci.,* **109,** 29 (1981).